Boxcar gating for time-resolved mid-infrared photothermal imaging of axon-bundle water boundaries

Panagis D. Samolis¹, Xuedong Zhu², Michelle Y. Sander^{1,3}

¹Department of Electrical and Computer Engineering and BU Photonics Center, Boston University, Boston, MA 02215

²Department of Biomedical Engineering, Boston University, Boston, Massachusetts 02215, USA

³Division of Materials Science and Engineering, Boston University, Brookline, MA 02446

*Corresponding author: psamolis@bu.edu, msander@bu.edu

Abstract: Time-resolved mid-infrared photothermal imaging via boxcar gating is presented for the study of interface dynamics between axon bundles and the surrounding water. © 2023 The Authors

1. Introduction

Water as an embedding medium is often avoided in IR imaging since it features a strong background absorption. However, the photothermal effects attributed to water absorption play a significant role in the generation of electrophysiological signals. While mid-infrared photothermal imaging has seen great progress in recent years [1], [2], [3] images of Amide I protein signatures of cells which feature comparable signals to their water background have not been shown. We present a novel method for time-resolved imaging in a confocal mid-infrared photothermal microscope using boxcar gating to extract hyper-temporal image stacks of the heating and diffusion processes in water without the need for complex post-image processing. Further, the interface dynamics between extracted axon-bundles and the surrounding water environment are imaged and analyzed.

2. Experimental Setup and Results

A quantum cascade laser (QCL) tunable from 1576 – 1740 cm⁻¹ with a repetition rate of 100 kHz operates as the pump. A continuous wave 980 nm laser diode serves as a probe laser that detects the pump induced thermal lensing effect. As seen in Fig. 1(a) the pump beam illuminates the sample via a ZnSe refractive objective. Epi-detection is performed and the backscattered signal is focused on a Si photodetector before being coupled to a 600 MHz lock-in amplifier.

Lock-in detection enables VIPPS imaging (Vibrational Infrared Photothermal amplitude and Phase Signals imaging) where the amplitude and phase signals are simultaneously acquired, each providing information with respect to absorption and changes in the rate of heat transport, respectively [4]. Boxcar (BC) measurements allow the acquisition of localized time curves of the probe backscatter signal over one period. In addition, hyper-temporal image stacks are acquired by tuning the start time (tg) of the gate window with a fixed duration of 250 ns. Selecting a gate window that overlaps with peak signal can result in an enhancement of the signal-to-noise ratio (SNR) by a factor of 4.3 compared to conventional photothermal amplitude imaging (PTS) since the temporal periods with little significant signal are filtered out [5]. This is presented in Fig.1(b) for the case of a 500 nm PMMA bead in air.

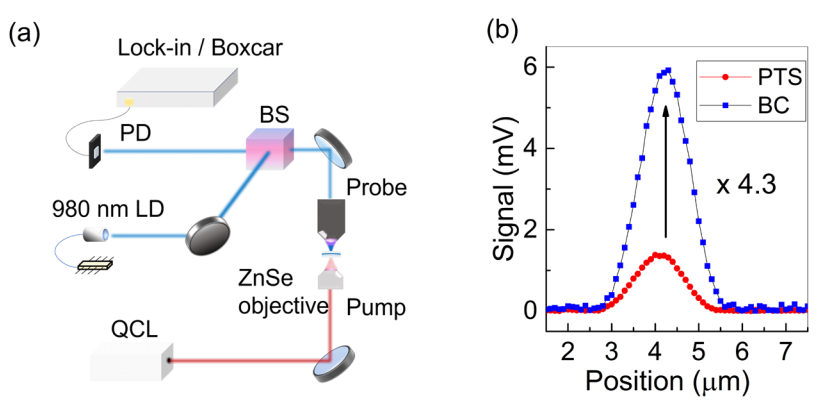


Fig. 1. (a) Experimental Setup. (b) 4.3 fold SNR enhancement from 68 to 296 of a 500 nm PMMA bead linescan with boxcar imaging at time of peak signal compared to standard PTS amplitude imaging.

An axon bundle (AB) consisting of multiple sensory and motor axons was extracted from the first pair of walking legs of a crayfish, dissected and isolated from the remaining tissue in physiological saline. The photothermal amplitude image was taken at a pump wavelength set to 1660 cm⁻¹, targeting the Amide I band. As shown in Fig. 2(a), there is a strong signal present from both the protein signatures in the interior as well as at the surrounding water. The phase

image, see Fig. 2(b), provides an enhanced contrast of the interface and both VIPPS images can be easily cross-registered with the optical microscope image, as presented in Fig. 2(c). Selected images from a hyper-temporal image stack of a 15 by 15 μ m area are presented in Fig. 2(d), capturing the interface between the axon-bundle and water. Specifically, the boxcar image at the time of peak signal (for t_g =0.5 μ s) and after 1.75 μ s of diffusion time (for t_g =2 μ s). A significant change in the signal distribution in the interior of the AB near the water interface is observed at the highlighted area (see white dashed box in Fig. 2(d)) when comparing the two images. Overall, it is observed that the signal is not smooth across the interface, but rather that characteristic gradients exist originating from thermal resistance effects at the boundary. To spatially map the different time decay constants, the coefficient of variance (CV) from the image time stack is plotted in Fig. 2(e). The CV is defined as the ratio of the standard deviation over the absolute value of the mean. The latter variable is correlated with the time decay and thus highlights areas with faster decay constants. The average CV value at the water background is 1.2. Enhancements with CV>1 are observed at the interface as well as in the interior of the axon bundle. In addition, areas with CV<1 are observed mostly in the AB interior. Three characteristic points are selected for each region of interest, specifically A1, A2 and water as denoted by the green, red and light blue dots in the CV image, respectively. The corresponding time curves are plotted in Fig. 2(f), characterized by material-specific time decay constants with τ_{d-A2} = 1.9 μ s > $\tau_{d-Water}$ = 1.5 μ s > τ_{d-A1} = 0.9 μ s.

In conclusion, this work addresses the gap of mid-infrared photothermal imaging in water by using the high contrast from interface thermal gradients as well as temporal imaging to identify areas with varying rates of decay. The ability to study the interfacial diffusion dynamics in such samples provides a useful tool to study the role of hydration in heat transfer and image local perturbations in neurological samples after IR illumination.

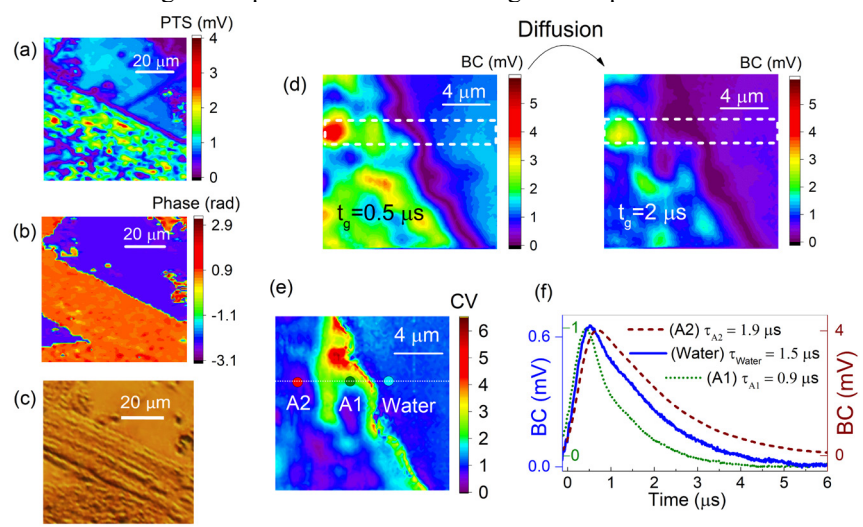


Fig. 2. (a) Photothermal amplitude, (b) phase and (c) optical microscope image of axon-bundle (AB) in water. (d) Selected images from a hypertemporal image stack of the AB water interface at time of peak signal (t_g =0.5 μ s) and after 1.75 μ s of diffusion time (t_g =2 μ s) where changes in the signal associated with the interior of the AB near interface are observed (see white dashed box). (e) The CV image allows extracting areas with faster decay constants (CV>1). (f) Time curves associated with points A2, A1 and water as marked in (e) with characteristic time decay constants.

This work was supported by National Science Foundation (NSF ECCS-1846659).

3. References

- S. Adhikari, P. Spaeth, A. Kar, M. D. Baaske, S. Khatua, and M. Orrit, "Photothermal Microscopy: Imaging the Optical Absorption of Single Nanoparticles and Single Molecules," ACS Nano 14, 16414–16445 (2020).
- J. Yin, L. Lan, Y. Zhang, H. Ni, Y. Tan, M. Zhang, Y. Bai, and J.-X. Cheng, "Nanosecond-resolution photothermal dynamic imaging via MHZ digitization and match filtering," Nat Commun 12, 7097 (2021).
- 3. M. Tamamitsu, K. Toda, H. Shimada, T. Honda, M. Takarada, K. Okabe, Y. Nagashima, R. Horisaki, and T. Ideguchi, "Label-free biochemical quantitative phase imaging with mid-infrared photothermal effect," Optica, OPTICA 7, 359–366 (2020).
- 4. P. D. Samolis, P. D. Samolis, D. Langley, D. Langley, B. M. O'Reilly, B. M. O'Reilly, Z. Oo, Z. Oo, G. Hilzenrat, G. Hilzenrat, S. Erramilli, S. Erramilli, S. Erramilli, S. Erramilli, A. E. Sgro, A. E. Sgro, A. E. Sgro, S. McArthur, S. McArthur, M. Y. Sander, M. Y. Sander, M. Y. Sander, and M. Y. Sander, "Label-free imaging of fibroblast membrane interfaces and protein signatures with vibrational infrared photothermal and phase signals," Biomed. Opt. Express, BOE 12, 303–319 (2021).
- 5. P. Fimpel, C. Riek, L. Ebner, A. Leitenstorfer, D. Brida, and A. Zumbusch, "Boxcar detection for high-frequency modulation in stimulated Raman scattering microscopy," Appl. Phys. Lett. 112, 161101 (2018).